

Characterization of the Deregulated Immune Activation Occurring at Late Stages of Mycobacterial Infection in TNF-Deficient Mice¹

Manuela Flório* and Rui Appelberg^{2*†}

In the absence of TNF, mice infected with *Mycobacterium avium* suffer a peculiar disintegration of the granulomas, with extensive apoptosis and necrosis of their cells, occurring during the course of the infection and leading to the death of the animals within a few days of its onset. The survival time depends on the virulence of the infecting strain as well as on the dose and route of infection. Intravenously infected mice developed the typical lesions in hepatic granulomas whereas aerosol-infected animals developed them in the lung granulomas. At the onset of the development of pulmonary granuloma disintegration, extensive expansion of T cells, with intense up-regulation of activation markers, massive exacerbation of their ability to secrete IFN- γ , and increased cytotoxic activity of both CD4⁺ and CD8⁺ T cells were observed. Forced expression of Bcl2 did not prevent the early death of infected TNF-deficient mice leading merely to a modest increase in survival times. The expression of the FasL on T cells was not affected but there was an intense up-regulation of the TRAIL in T cells and, in particular, myeloid cells. We thus show that an exacerbated immune response occurs in TNF-deficient hosts during *M. avium* infections that leads to enhanced IFN- γ production and late up-regulation of TRAIL which may contribute to granuloma disintegration. *The Journal of Immunology*, 2007, 179: 7702–7708.

Tumor necrosis factor has pleiotropic effects during mycobacterial infections. Thus, while rTNF can activate macrophages in vitro for enhanced control of mycobacterial growth (1, 2), neutralization of TNF leads to exacerbation of in vivo proliferation of mycobacteria either in mouse models of infection (3–5) or in human patients undergoing therapy with anti-TNF formulations (6). However, the in vivo role of TNF is more complex than simply the activation of macrophages. TNF regulates leukocyte recruitment and inflammation and is required for the organization of the granuloma (3, 7–9) as well as for its maintenance (10, 11). In fact, in the absence of TNF signaling through its type 1 receptor (TNFR1), mice infected with mycobacteria show granuloma disintegration characterized by extensive cellular apoptosis and necrosis within the granulomas (10, 12–17). In some cases, this phenomenon underlies the premature death of mice which, otherwise, would still be able to cope with the mycobacterial burden (9, 10). It is unclear what is the basis of this acute cell death occurring on an established, chronic granuloma. When infected mice become moribund, they exhibit a dramatic increase in IFN- γ production by T cells which is dependent on IL-12p40 (10,

18). TNF may thus be pivotal in keeping the activation of T cells under control and avoid this explosive secretion of IFN- γ . Alternatively, TNF may provide survival signals to leukocytes and prevent their demise as it is known that TNF can lead to activation of NF- κ B and promote the transcription of antiapoptotic factors (19) which might be required to maintain the viability of leukocytes inside granulomas. In addition, TNF has been shown to inhibit the production of IL-12 and IL-23 by macrophages and dendritic cells (20). Thus, in its absence, a deregulated activation of Th1 cells may lead to extensive immune activation and promotion of pathology. It was shown that neutralization of IL-12 or IFN- γ as well as depletion of CD4⁺ T cells was able to prevent the disintegration of granulomas and the death of TNFR1-deficient mice infected with *Mycobacterium avium*, showing that hypersecretion of IFN- γ by the latter T cell population may be the final mediator in the induction of this type of pathology (11). IFN- γ has likewise been implicated as a primary mediator of other immunopathological conditions associated to chronic mycobacteriosis such as the induction of caseous necrosis in granulomas and the development of severe lymphopenia (21–23). However, the immediate effector mechanisms have not been identified for any of these phenomena. In this study, we use TNF-deficient mice to further dissect the granuloma disintegration already described in the literature. We favored an aerogenic infection to more easily access leukocytes from the affected tissue, the lung. We thus extend our knowledge on this phenomenon by reporting the extensive activation of T cells in the lungs of aerogenically infected TNF-deficient mice and the up-regulation on the surface of leukocytes of a death-inducing ligand, TRAIL.

Materials and Methods

Mice and infection

Female C57BL/6 mice were purchased from Harlan Iberica. C57BL/6.TNF^{-/-} (B6.TNF^{-/-}) mice were purchased from B&K Universal and bred in our facilities. Heterozygous transgenic mice overexpressing one copy of human BCL2 in the hemopoietic cell lineage (C57BL/6.Bcl2^{0/+})

*Laboratory of Microbiology and Immunology of Infection, Instituto de Biologia Molecular e Celular, and [†]Instituto de Ciências Biomédicas de Abel Salazar, University of Porto, Porto, Portugal

Received for publication July 17, 2007. Accepted for publication September 19, 2007.

The costs of publication of this article were defrayed in part by the payment of page charges. This article must therefore be hereby marked *advertisement* in accordance with 18 U.S.C. Section 1734 solely to indicate this fact.

¹ This work was supported by Grants POCTI/32629/99 and PSIDA/MGI/49647/2003 from the Portuguese Science and Technology Foundation (FCT; Portugal) and SDH.IC.L01.15 from the Calouste Gulbenkian Foundation (Portugal). M. F. received a fellowship from the FCT.

² Address correspondence and reprint requests to Dr. Rui Appelberg, Laboratory of Microbiology and Immunology of Infection, Institute for Molecular and Cell Biology, Rua do Campo Alegre 823, 4150-180 Porto, Portugal. E-mail address: rappelb@ibmc.up.pt

Copyright © 2007 by The American Association of Immunologists, Inc. 0022-1767/07/\$2.00

were supplied by J. Adams (Walter and Eliza Hall Institute of Medical Research, Melbourne, Australia) and were bred in our facilities. They were crossed with TNF mice to obtain B6.TNF^{-/-}Bcl2^{0/+} mice. Mice were infected either by the i.v. route by injecting 10⁶ CFU of *M. avium* strains 1983, 2447, or ATCC 25291 (American Type Culture Collection) or 10² CFU of strain 25291, or aerogenically by being exposed to an aerosolized suspension of *M. avium* strain 2447 using a Glas-Col Inhalation Exposure System: a 7 × 10⁷ CFU/ml suspension resulted in the implantation of ~900 CFU of mycobacteria in the lungs of each mouse and a 7 × 10⁸ CFU/ml suspension led to the implantation of ~2000 CFU per mouse. Survival of the infected mice was followed in one cohort of infected animals whereas the course of the infection was followed in a parallel group of mice by performing viable counts of the mycobacteria in the infected organs following their homogenization and serial dilution plating onto Middlebrook 7H10 medium (Difco). Bacterial inocula were prepared as previously described (24).

Study of immune cells

For the isolation of lung cells, blood was washed from the lungs by perfusing 10 ml of HBSS through the heart. Lungs were aseptically removed, the tissue was finely sliced with a razor blade and incubated at 37°C for 60 min in 10 ml of DMEM with 10% FCS (DMEM/10% FCS; Invitrogen Life Technologies) in the presence of collagenase (Sigma-Aldrich) at a final concentration of 100 U/ml. Undigested tissue was then forced through a 70-μm nylon cell strainer. Single-cell suspensions from spleens were prepared by teasing portions of spleen with forceps in DMEM supplemented with 10% FCS. Cells (from lung or spleen) were pelleted by centrifugation, washed, and incubated with NH₄Cl hemolytic buffer to lyse any remaining erythrocytes. Cell suspensions were then washed with HBSS and resuspended in DMEM/10% FCS.

For in vitro stimulation studies, cells were cultivated at a density of 2 × 10⁵ cells/well in a U-bottom, 96-well cell culture plate and incubated in triplicate in DMEM with 10% FCS with no further stimulus or in the presence of mycobacterial envelope proteins at a final concentration of 4 μg/ml. Supernatants from the cultures were collected after 72 h of culture, and the IFN-γ was produced was quantified by a two-site sandwich ELISA method, using anti-IFN-γ specific, affinity purified mAbs (R4-6A2 as capture and biotinylated AN-18 as detecting Ab) and a standard curve generated with known amounts of recombinant murine IFN-γ (Genzyme). The same method was used to quantify the amount of IFN-γ present in the serum of the infected mice. Mycobacterial envelope proteins were prepared from *M. avium* broth cultures as described previously (24).

Flow cytometry

For the immunofluorescence staining, 10⁶ cells were incubated in a 96-well microtiter plate with fluorochrome-conjugated Abs. All Abs were from BD Pharmingen with the exception of the Ab anti-TRAIL that was acquired from Abcam and were used at the dilutions recommended by the manufacturers. The cells were washed twice with PBS containing 3% FCS; propidium iodide (Sigma-Aldrich) was added to the cells at a final concentration of 1 μg/ml to allow the exclusion of dead cells.

For the analysis of IFN-γ production, lung cells were cultured in DMEM supplemented with 10% FCS at a density of 1 × 10⁶ cells/ml and incubated for 2 h at 37°C in the presence of PMA (Sigma-Aldrich) plus ionomycin (Calbiochem) at a final concentration of 25 μg/ml each followed by an incubation of 2 h in the presence of 0.01 mg/ml brefeldin A (Sigma-Aldrich). After extensive washing with ice-cold PBS, cells were labeled with FITC-conjugated anti-CD4 or with FITC-conjugated anti-CD8 and fixed for 20 min in a 2% paraformaldehyde solution. The fixed cells were then washed, permeabilized for 10 min at room temperature with PBS/1% FCS/0.1% Na₂S₂O₈/0.5% saponin, and incubated with 5 μg/ml PE-conjugated anti-IFN-γ mAb for 20 min at room temperature. The analysis of the stained cell populations was based on the acquisition of 10,000 events in a FACSort (BD Biosciences) equipped with CellQuest and Flow Jo software.

Cytotoxicity assay

Cells of the P815 mastocytoma cell line (ATCC) were used as targets in this assay. Cells were harvested from an exponentially growing culture, labeled by incubation with 200 μCi of ⁵¹Cr-sodium dichromate (Amersham) at 37°C for 2 h. After extensive washing, the cells were incubated with anti-CD3 mAb or with hamster IgG at a concentration of 30 μg/ml for 20 min. A total of 5 × 10³ target cells were plated in a U-bottom 96-well cell culture plate and different ratios of effector cells were added in triplicate. After 6 h of culture at 37°C in a CO₂ atmosphere, 150 μl of supernatant was collected and isotope release was measured in a Microbeta Trilux scintillation counter (PerkinElmer). Spontaneous ⁵¹Cr release was

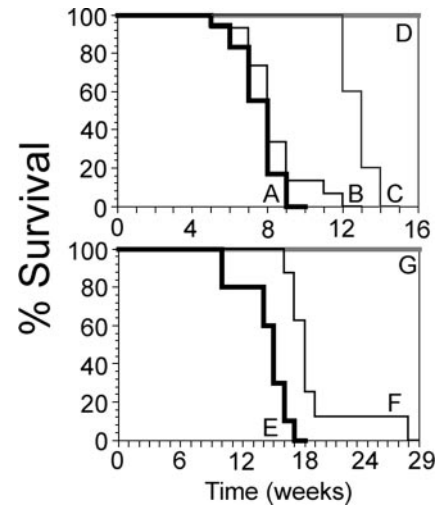


FIGURE 1. Decreased survival of TNF-deficient mice infected with *M. avium*. TNF^{-/-} mice were infected i.v. with 10⁶ CFU of *M. avium* ATCC 25291 (A, thick black line) or 2447 (B, thin black line), or with 100 CFU of *M. avium* ATCC 25291 (C, thin gray line) (top graph), or were infected with aerosolized *M. avium* 2447 at a concentration of 10⁷ (E, thick black line) or 10⁸ (F, thin black line) CFU/ml (bottom graph). Survival of control C57BL/6 mice infected in the same way is represented by the thick gray lines (D and G) and was 100% during the time frame of the studies in all experiments.

measured by incubation of target cells in DMEM in the absence of effector cells and total release was measured by incubation of target cells with 10% saponin. Specific cytotoxicity was calculated as percent lysis = (A - B)/(C - B) × 100, where A is the experimental release, B is the spontaneous release, and C the total release. Purified CD4⁺ or CD8⁺ T cells that were in some cases used as effector cells for the cytotoxicity assay were obtained by cell sorting from pooled lung cell suspensions using a FACSAria cell sorter (BD Biosciences).

Histology

Lungs were fixed in buffered formaldehyde, embedded in paraffin, and sections were stained with H&E for histological analysis.

Statistical analysis

The Student *t* test was used to compare paired data and the log-rank test was used to compare survival times.

Results

TNF-deficient mice have reduced survival during *M. avium* infections when compared with control C57BL/6 animals

The survival of the *M. avium*-infected TNF-deficient mice varied according to the dose and route of infection and virulence of *M. avium* isolate. Intravenous infection with high doses (10⁶ CFU) led to the earliest mortality in the case of strains ATCC 25291 (mean survival time (MST)³ = 57.5 ± 8.4 days) and 2447 (MST = 61.3 ± 12.3 days) (Fig. 1), although TNF-deficient mice infected with a low virulence strain (strain 1983) survived longer than 400 days (data not shown). Infection with a lower inoculum dose of *M. avium* ATCC 25291 (10² CFU) led to a later death of B6.TNF^{-/-} mice (MST = 94.0 ± 4.3 days) as compared with the high dose. In contrast, C57BL/6 mice survived longer than 90 days (high dose of strain ATCC 25291), 330 days (strain 2447), or 200 days (low dose of strain ATCC 25291). Aerosol infection was also established with strain 2447 (Fig. 1) leading to mean survival times of 146.6 ± 27.3 days for the lower dose and 118.5 ± 41.5 days for

³ Abbreviations used in this paper: MST, mean survival time; BCG, bacillus Calmette-Guérin.

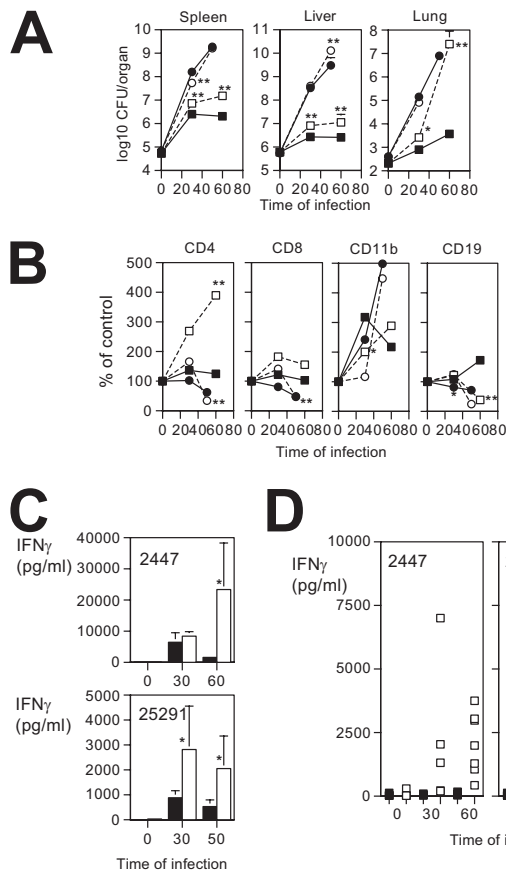


FIGURE 2. Characterization of the infection and immune response following an i.v. challenge of C57BL/6 mice and B6.TNF^{-/-} mice with *M. avium* ATCC 25291 (circles) or 2447 (squares). **A**, *M. avium* growth in the lungs of control C57BL/6 animals (closed symbols) and of B6.TNF^{-/-} mice (open symbols). **B**, Variation in the number of splenic cells expressing CD4, CD8, CD11b, or CD19 in the infected animals relative to the cell numbers of control uninfected mice (plotted as 100%). **C**, IFN- γ secreted by spleen cells from C57BL/6 (■) or B6.TNF^{-/-} (□) mice infected with *M. avium* 2447 (top graph) or ATCC 25291 (bottom graph) after stimulation for 72 h with *M. avium* Ag. **D**, Amounts of IFN- γ detected in individual sera from infected C57BL/6 (closed symbols) or B6.TNF^{-/-} (open symbols) mice. Time of infection is shown in days.

the higher dose, compared with no deaths in C57BL/6 mice infected for up to 250 days. These data suggest that the intensity of the immunological stimulus underlies the mortality in TNF-deficient hosts. Therefore, we next characterized the mycobacterial growth and the immune responses in these infections.

TNF-deficient mice have an exacerbated immune response to *M. avium* infections when compared with control C57BL/6 animals

Following i.v. infection with 10⁶ CFU, strain 2447 proliferated more extensively in TNF-deficient mice than in control mice (Fig. 2A). Strain ATCC 25291, however, proliferated equally well in both mouse strains (Fig. 2A). CD4⁺ and CD8⁺ T cells expanded more vigorously in TNF-deficient mice than in C57BL/6 controls, particularly in the case of strain 2447 (Fig. 2B). As already described, strain ATCC 25291 led to lymphopenia at the late stages of infection, thus limiting the expansion of the T cells. The accumulation of CD11b⁺ myeloid cells was smaller in the TNF-deficient hosts than in the control animals and B cells showed extensive elimination at late time points of infection in the TNF-deficient mice as compared with small alterations in number in the controls (Fig. 2B). Spleen cells from infected B6.TNF^{-/-} mice responded more intensely to my-

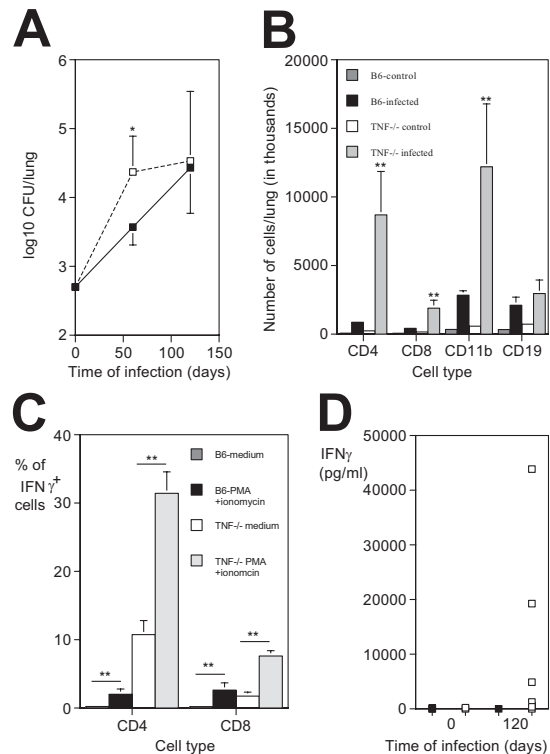


FIGURE 3. Characterization of the pulmonary infection and immune response following aerosol challenge of C57BL/6 mice and B6.TNF^{-/-} mice with *M. avium* 2447. **A**, *M. avium* growth in the lungs of control C57BL/6 animals (closed symbols) and of B6.TNF^{-/-} mice (open symbols). **B**, Number of cells expressing CD4, CD8, CD11b, or CD19 in uninfected animals and in mice infected for 120 days with an aerosol of *M. avium* as determined by flow cytometric analysis of cells isolated from dissociated lung tissue. **C**, Flow cytometric analysis of IFN- γ -expressing CD4⁺ or CD8⁺ cells with or without stimulation by PMA and ionomycin, at day 120 of infection. **D**, Amounts of IFN- γ detected in individual sera from infected C57BL/6 (closed symbols) or B6.TNF^{-/-} (open symbols) mice.

cobacterial Ags than cells from infected controls with regards to IFN- γ secretion (Fig. 2C). IFN- γ levels were higher in the case of the cell cultures from mice infected with strain 2447 than strain ATCC 25291, correlating well with the higher numbers of T cells

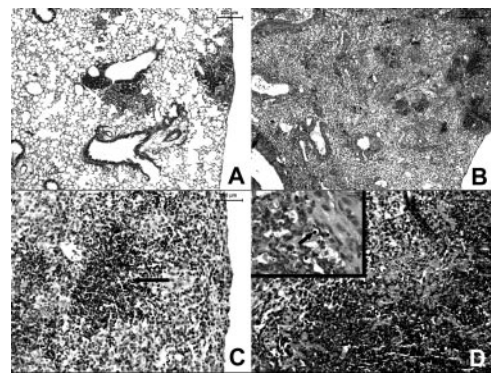


FIGURE 4. Histological evidence of granuloma disintegration in the lungs of TNF-deficient mice infected with an aerosol of *M. avium* 2447. **A**, Lesions in the lungs of a C57BL/6 mouse infected for 240 days with *M. avium*. **B**, Lung section of a moribund TNF^{-/-} mouse infected for 135 days with *M. avium*. **C**, Higher magnification of the previous sample showing the mononuclear infiltrate and a nest of lymphocytes (arrow). **D**, Another field of the same sample where extensive disintegration of the cellular infiltrates is occurring. *Inset*, Several pyknotic nuclei within the area.

Table I. Effects of BCL2 overexpression on the course of an i.v. infection of TNF-deficient mice^a

Infection	Mouse Strain	Log CFU (Spleen)	Log CFU (Liver)	Log CFU (Lung)	CD4 ⁺ Cells × 10 ⁻⁶ (Fold-Increase) ^b	IFN-γ (ng/ml) ^c
45 days with strain 25291	TNF ^{-/-}	8.9 ± 0.3	9.7 ± 0.4	6.9 ± 0.9	23.5 ± 18.5 (2.2-fold)	11.4 ± 7.4
	TNF ^{-/-} Bcl2 ^{0/tg}	8.2 ± 0.5*	9.0 ± 0.2*	6.4 ± 0.5	119.8 ± 102.8 (2.5-fold)	9.0 ± 6.6
60 days with strain 2447	TNF ^{-/-}	6.7 ± 0.3	7.1 ± 0.8	6.4 ± 0.7	31.5 ± 12.1 (3.0-fold)	38.1 ± 17.2
	TNF ^{-/-} Bcl2 ^{0/tg}	6.2 ± 0.3*	6.6 ± 0.3	4.8 ± 0.7**	211.4 ± 124.3** (5.2-fold)	18.0 ± 8.2*

^a Statistical analysis of the differences between B6.TNF^{-/-} and B6.TNF^{-/-}Bcl2^{0/tg} mice was done using the Student *t* test and the significant differences are labeled: *, *p* < 0.05 and **, *p* < 0.01.

^b Number of CD4⁺ cells in the spleen of infected mice and fold-increase in their number relative to noninfected animals (in parentheses).

^c Concentration of IFN-γ in the supernatants of cultures of spleen cells from infected animals stimulated for 72 h with *M. avium* Ag.

in this infection. Finally, sera from infected B6.TNF^{-/-} mice had dramatically increased amounts of IFN-γ as compared with sera from infected C57BL/6 controls (Fig. 2D). As previously reported by Ehlers et al. (10), infected moribund TNF-deficient mice exhibited numerous granulomas within the liver tissue undergoing disintegration, with many necrotic areas and evidence of apoptotic cells (data not shown). Such pathology was not detected in other organs such as the spleen and the lung, also targets of infection.

A similar analysis was performed in mice infected with strain 2447 through the aerogenic route. As shown in Fig. 3A, there was a transient exacerbation in growth of *M. avium* in the lungs of B6.TNF^{-/-} mice at day 60 of infection but the numbers of mycobacteria were similar in both strains of mice at a time when the B6.TNF^{-/-} mice were becoming moribund. The accumulation of leukocytes in the lungs was also studied following their isolation from digested pulmonary tissue and showed that B6.TNF^{-/-} mice infected for 120 days had considerably more CD4⁺, CD8⁺, and CD11b⁺ cells than control C57BL/6 mice infected for the same period of time (Fig. 3B). T cells

from these infected B6.TNF^{-/-} mice showed a higher percentage of IFN-γ-positive cells than T cells from infected controls, particularly with regards to the CD4⁺ population of cells (Fig. 3C). The latter data correlated well with the increased levels of serum IFN-γ detected at 120 days of infection in B6.TNF^{-/-} mice as compared with control C57BL/6 mice (Fig. 3D). Even at 240 days of infection, when all infected TNF-deficient mice had died, infected C57BL/6 mice had only a small number of discrete lesions in their lungs (Fig. 4A). In contrast, the lungs of moribund TNF-deficient mice infected with strain 2447 showed massive infiltration of the whole lung frequently with little remaining uninvolved alveolar tissue (Fig. 4B). This infiltration consisted of mononuclear cells with many foci of lymphocyte accumulation (Fig. 4C) and areas of necrotic tissue (Fig. 4D) where apoptotic cells with pyknotic nuclei were identified (Fig. 4D, inset). It was interesting to find no granuloma disintegration in the livers of the same animals whereas that was the site where such pathology developed when the infection was initiated through the i.v. route (data not shown).

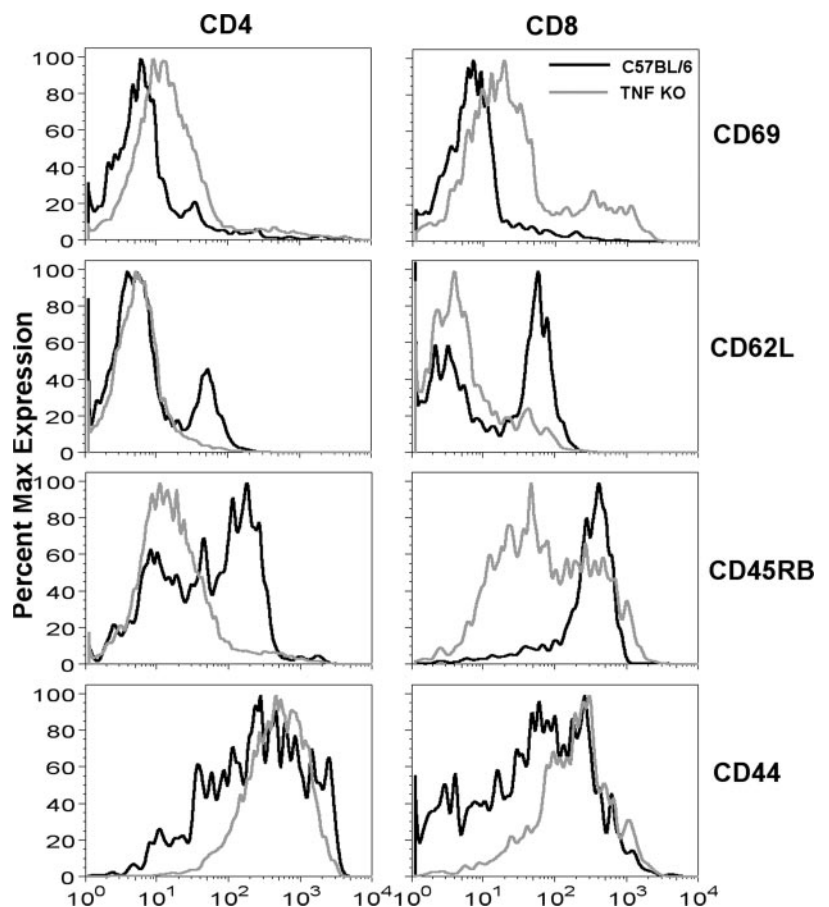


FIGURE 5. Evidence for extensive T cell activation in the lungs of TNF-deficient mice infected for 120 days with an aerosol of *M. avium* 2447. Expression of CD69, CD62L, CD45RB, and CD44 was evaluated on gated CD4⁺ or CD8⁺ cells (C57BL/6, black lines; B6.TNF^{-/-}, gray lines). Histograms show the distribution of cells as the percentage of the maximum value using the concatenated results of data from seven animals per group except for CD44 where four animals were analyzed.

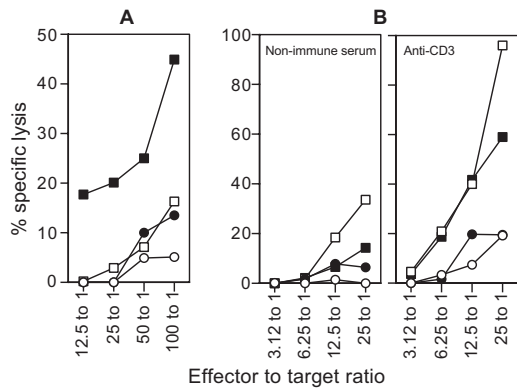


FIGURE 6. Increased T cell cytotoxicity against target P815 cells in TNF-deficient infected mice. *A*, Cytotoxicity of spleen cells from infected C57BL/6 (circles) or B6.TNF^{-/-} (squares) in the absence (open symbols) or presence (closed symbols) of anti-CD3 Abs. *B*, Cytotoxicity of purified CD4⁺ (open symbols) or CD8⁺ (closed symbols) T cells from infected C57BL/6 (circles) or B6.TNF^{-/-} (squares) mice in the absence (*left*) or presence (*right*) of anti-CD3 Abs. Data are representative of three independent experiments.

Bcl2 overexpression slightly improves survival during *M. avium* ATCC 25291 infections when compared with control C57BL/6 animals

Given the suggestion of apoptotic events taking place before the demise of the infected TNF-deficient mice, we studied the infection in mice lacking TNF but overexpressing the antiapoptotic molecule BCL2. TNF-deficient mice overexpressing *Bcl2* were infected in parallel with TNF-deficient mice, and survival after i.v. *M. avium* infection was analyzed. B6.TNF^{-/-} mice survived for 75.4 ± 14.9 days and 47.2 ± 9.0 days following infection with strains 2447 and ATCC 25291, respectively, whereas B6.TNF^{-/-} Bcl2^{0/+} mice had increased survival times of 84.8 ± 15.2 days ($p = 0.28$ according to the log-rank test) and 68.1 ± 10.4 days ($p < 0.001$ according to the log-rank test), respectively. Control B6.Bcl2^{0/+}, like control B6 mice, survived longer than 330 days when infected with strain 2447 and longer than 90 days when infected with strain ATCC 25291. Data from infected mice close to the time of death is presented in Table I. Thus, the transgene conferred partial resistance to infection associated with an increase in the number of cells, which was already apparent in noninfected animals. Thus, CD4⁺ T cell numbers at 45 days of infection with *M. avium* 25291 were increased 2.2-fold in TNF-deficient mice and 2.5-fold in TNF-deficient mice overexpressing Bcl2 relative to uninfected controls. In contrast, the expansion of this cell subset was larger in *Bcl2*-transgenic B6.TNF^{-/-} mice (5.2-fold) as compared with the B6.TNF^{-/-} animals (3.0-fold) during a 60 days infection by *M. avium* 2447. We have previously found (Ref. 21 and data not shown) that such expansion during infection with either strain ATCC 25291 or strain 2447 did not occur in control C57BL/6 mice even when overexpressing Bcl2 at such time points. The larger expansion of the T cells in the case of the infection by strain 2447 may have counteracted the protective effects of Bcl2 on the survival during infection by *M. avium* 2447 by providing a bigger number of offending T cells (a statistically nonsignificant 10-day increase in survival time was found). In contrast, the balance between the expansion of T cells due to the forced expression of *Bcl2* and the development of lymphopenia caused by the infection made the increase in survival bigger and statistically significant in the case of the infection by *M. avium* 25291 (around 21 days). In both instances, the IFN- γ response remained exacerbated as compared with the responses found in C57BL/6 animals. Thus,

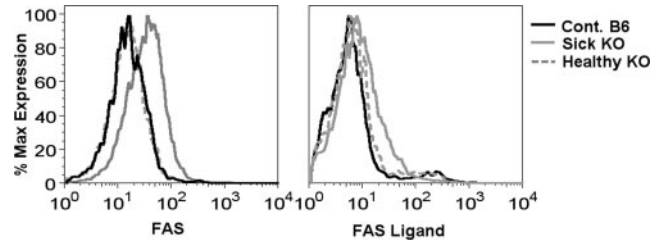


FIGURE 7. Expression of CD95 (Fas) and CD154 (FasL) on CD3⁺ cells from C57BL/6 (black lines) and B6.TNF^{-/-} (gray lines) mice infected for 120 days with *M. avium* 2447. The latter mice were separated into two groups: one appeared healthy (broken lines) whereas the other included mice with signs of sickness (see *Results*). Three animals per group were studied for the three groups.

spleen cells from TNF-deficient mice and Bcl2-transgenic TNF-deficient mice infected with strain ATCC 25291 secreted 11.4 ± 7.4 ng of IFN- γ /ml and 9.0 ± 6.6 ng of IFN- γ /ml, respectively (Table I) whereas C57BL/6 controls, overexpressing Bcl2 or not, always secreted <1 ng of IFN- γ /ml at day 60 of infection (21). Overexpression of Bcl2 more than doubled the amounts of IFN- γ secreted by spleen cells of C57BL/6 mice infected for 60 days with strain 2447 (20.3 ± 3.3 ng of IFN- γ /ml in Bcl2 transgenic as compared with 7.8 ± 2.2 ng of IFN- γ /ml in nontransgenic C57BL/6). However, the values were higher in the case of TNF-deficient (38.1 ± 17.2 ng of IFN- γ /ml) than in Bcl2-transgenic TNF-deficient (18.0 ± 8.2 ng of IFN- γ /ml) mice infected for 60 days with strain 2447.

T cells in the lungs of infected TNF-deficient mice exhibit an enhanced activated phenotype and increased cytotoxicity

To characterize further the cells in the lesions of moribund animals and find clues to the mechanisms leading to the demise of the

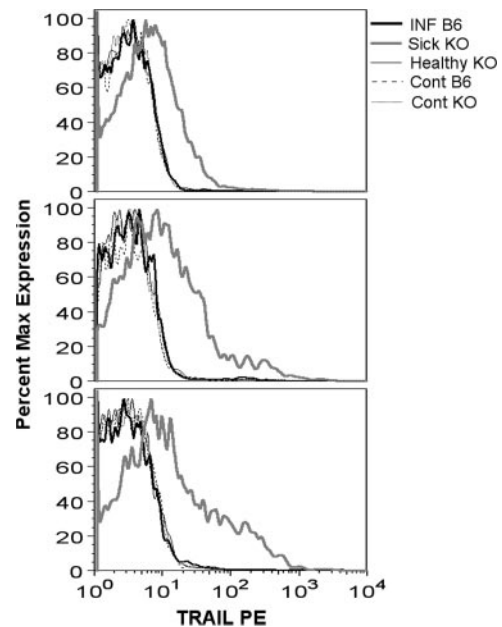


FIGURE 8. Increased expression of TRAIL in CD4⁺, CD8⁺, and CD11b⁺ cells in the lungs of C57BL/6 (black lines), healthy looking B6.TNF^{-/-} (thin lines), or sick B6.TNF^{-/-} (thick gray lines) mice infected for 120 days with an aerosol of *M. avium* 2447. Control not-infected C57BL/6 (dashed lines) or B6.TNF^{-/-} (dotted lines) mice are also shown. Histograms were normalized for the different number of events by converting data into percentage of maximum number of events. Each histogram is representative of a group of five or six samples.

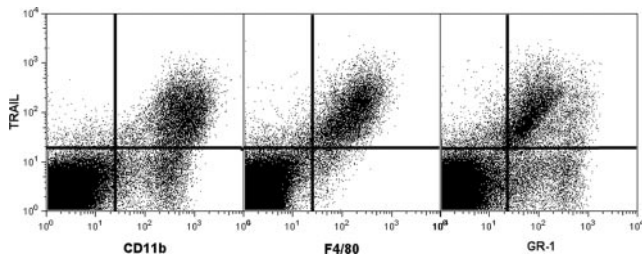


FIGURE 9. Dot-plot representation of the FACS analysis of lung cells from an infected moribund B6.TNF^{-/-} mouse. Cells were stained for the markers CD11b, F4/80, and Gr1 and for TRAIL. This pattern is representative of all animals tested.

TNF-deficient animals, we selected the aerogenic infection model given that the isolation lung cells were easier than that of the liver granulomas cells. Given the extensive accumulation of lymphocytes, namely T cells in those lesions, we analyzed by flow cytometry the activation of those T cells. As shown in Fig. 5, CD4⁺ and CD8⁺ T cells from TNF-deficient animals had increased expression of the early activation marker CD69, and of CD44, while down-regulating more extensively the molecules CD62L and CD45RB as compared with control C57BL/6 animals. All these alterations suggested an increased activation of the T cells. We also studied the cytotoxic activity of T cells. As shown in Fig. 6, either whole T cells or purified CD4⁺ or CD8⁺ T cells from TNF-deficient mice exhibited increased anti-CD3-triggered cytotoxicity against P815 targets as compared with cells from C57BL/6 mice.

Inflammatory cells in the lungs of moribund mice up-regulate TRAIL

To understand the mechanisms of the cellular death occurring in the granulomas of moribund TNF-deficient mice, we analyzed the expression of death-inducing molecules on the surface of lung leukocytes. When we stained cells for the expression of FasL or FasR, no important differences were observed between cells of either strain (Fig. 7). We thus looked at an additional death-inducing molecule, TRAIL. Lung cells from noninfected mice or from infected C57BL/6 animals did not express TRAIL (Fig. 8). Expression of TRAIL was increased in CD4⁺ and CD8⁺ T cells of TNF-deficient mice but only when they started to look clinically ill (Fig. 8). Additionally, an increase in expression was found on another cell subset which we identified as CD11b⁺ cells (Fig. 8). To better characterize this cell type that was the predominant cell expressing TRAIL, we performed additional phenotypic characterization. This TRAIL expressing population present in infected and moribund B6.TNF^{-/-} mice was found to be CD11b⁺, F4/80⁺, and expressed intermediate amounts of Gr1 (Ly6C/G) (Fig. 9) typical of a subset of macrophages found to accumulate in other infectious models (25, 26).

Discussion

The availability of genetically engineered mice lacking the type 1 TNFR (TNFRp55^{-/-}) or TNF itself has allowed the analysis of the role played by this cytokine in resistance to mycobacterial infections. Initial studies highlighted the importance of TNF in a mouse model of disseminated tuberculosis infection (12). Intravenously infected TNFRp55^{-/-} mice showed severe pathology in *Mycobacterium tuberculosis*-infected organs while presenting increased bacterial loads and decreased survival (12). Similar exacerbation of infection with concomitant development of necrotic pathology was observed in models of *Mycobacterium bovis* bacillus Calmette-Guérin (BCG) infection of TNF-deficient and TNF/lymphotoxin-deficient mice (13–16). Transgenic mice overex-

pressing a soluble form of the type 1 TNFR became similarly more susceptible to either *M. tuberculosis* or BCG again exhibiting higher bacterial loads and developing caseous necrosis (17). These examples associated increased mycobacterial proliferation with development of pathology. In contrast, a model of infection by virulent *M. avium* has allowed Ehlers et al. (10, 11) to describe the development of granuloma disintegration and early mortality in infected TNFR1-deficient animals without concomitant exacerbation in mycobacterial loads during infection. It became clear that most of the pathology stemmed not from the increased numbers of mycobacteria but most likely from a deregulation of the immune response to infection. This phenomenon was also well-characterized by Zganiacz et al. (16) in their model of BCG infection. Here, we further dissected the *M. avium* model and 1) we show that the development of immunopathology is not due to an imbalance in the signaling between the two TNFRs but rather to an absence of signaling through the type 1 receptor, 2) we confirm the exacerbated immune responses that take place in the absence of TNF signaling and that likely underlie the development of the immunopathology, i.e., granuloma disintegration, and 3) we show that the site of the immunopathology depends on the route of infection; it occurs in the liver following an i.v. infection but it is found in the lung when the animals are infected with an aerosol. In any case, both situations lead to the early death of the animals which is not strictly dependent on mycobacterial loads as in other mycobacteriosis, because moribund B6.TNF^{-/-} mice had similar loads as healthy looking C57BL/6 mice that went on to survive several weeks or months longer. Curiously, death of B6.TNF^{-/-} mice occurred at roughly the same time point of infection following an i.v. infection with the highly virulent strain ATCC 25291 as with the less virulent strain 2447, despite the former infection leading to much heavier mycobacterial loads than the latter. This may relate to the fact that the highly virulent strain causes lymphopenia and, in some way, dampens the exacerbated immune response that ensues in the absence of TNF. This interpretation may also explain why overexpression of BCL2 in hemopoietic cells protects slightly better in the case of infection of TNF-deficient mice infected with strain ATCC 25291 than with strain 2447. In fact, in the latter case, increased BCL2 expression leads to an infection-dependent 5-fold increase in CD4⁺ T cell numbers as compared with only 3-fold in nontransgenic mutants, thus further increasing the numbers of the cellular culprit of the increased mortality. In contrast, given the depletion of T cells observed during infection with strain ATCC 25291, infection of either *bcl2*-transgenic or nontransgenic mutant mice led to similar 2- to 2.5-fold increases in T cell numbers. This allows us to state that in the presence of similar numbers of offending T cells, BCL2 can partially counteract the apoptotic phenomena induced and delay the time of death.

Previous work from our laboratory has shown that chimeric mice whose TNFR1 deficiency was limited to the lymphoid lineage did not develop granuloma disintegration as mice lacking the receptor in all cell types did (21). This means that the cell type regulated by TNF is most likely of myeloid origin. The observation that TNF can dampen the secretion of IL-12 by APCs (20) is in line with these data and suggests that myeloid cells become uncontrollably stimulated during mycobacterial infection and overproduce cytokines that will activate T cells in an exaggerated fashion. Here, we present evidence that TNF-deficient mice, in contrast to control C57BL/6 mice, accumulate massive numbers of CD4⁺ T cells in their lungs during infection and that all these cells show evidence of activation (all up-regulate CD44 and down-regulate CD45RB and CD62L). Even the expression of CD69, a transient early marker of activation easily detected in vitro but seldom found

up-regulated *in vivo*, is increased in T cells from infected TNF-deficient hosts. In addition to CD4⁺ cells, CD8⁺ T cells also followed the same trends of activation. Among the products of the T cells, IFN- γ is of pivotal importance for the disintegration of the granulomas as the studies of Ehlers et al. (11) have demonstrated. This increase in the ability to secrete IFN- γ was also found in all our models. Instead of picogram amounts of this cytokine, we generally detected nanogram amounts at late stages of the infection in B6.TNF^{-/-} mice, clearly illustrating the deregulation of the immune response in these animals. Less clear is the relevance of other T cell functions, such as cytotoxicity which was found enhanced in T cells from B6.TNF^{-/-} mice, as compared with control C57BL/6 animals.

It is still not known how the increased amounts of IFN- γ produced in the absence of TNF regulation might lead to the immunopathology. Other models have linked IFN- γ to other immunopathological consequences of *M. avium* infection but the mechanisms involved have not been identified (21–23). We show here that one of the consequences of the deregulated response is the expression of TRAIL in T cells and, with more intensity, in CD11b⁺F4/80⁺Gr1^{int} macrophages. Whether this cell type is the final mediator of cell death within the granuloma is yet unclear and this issue will require further studies, namely the use of TRAIL-deficient mice and crosses with the TNF-deficient animals. Also unknown is whether TRAIL up-regulation might be a consequence of IFN- γ activation or, indirectly, of a response to another mediator induced by IFN- γ . Because it is known that TRAIL expression can be increased by type I IFNs (27), the following scenario can be envisaged. In the absence of regulatory TNF, APCs are stimulated by mycobacterial products to produce heightened amounts of co-stimulatory cytokines such as IL-12. These, in turn, lead to increased priming of CD4⁺ T cells that will secrete massive amounts of IFN- γ . Upon reaching a certain threshold, this cytokine will promote the expression of apoptosis-inducing molecules on the surface of macrophages (and maybe other cell types). We speculate that it will be the increased expression of the latter molecules that will eventually trigger the death of the cells within the granuloma leading to organ failure (be it the liver upon *i.v.* infection or the lung upon an aerogenic challenge) and the demise of the infected host. Because TRAIL up-regulation is a terminal phenomenon occurring in already moribund animals, it is unlikely that this molecule contributes to the immune activation which is observed to increase steadily from the beginning of the infection. Instead, as stated already, it is more likely that TRAIL expression is itself the result of such exacerbated immune response. Future studies will address different steps in this hypothetical sequence of events.

Acknowledgments

We are indebted to Alexandra Réma, Fátima Faria, and Célia Lopes for their technical help and to Nuno Lunet and Henrique Barros for statistical analysis.

Disclosures

The authors have no financial conflict of interest.

References

- Bermudez, L. E. M., and L. S. Young. 1988. Tumor necrosis factor, alone or in combination with IL-2, but not IFN γ , is associated with macrophage killing of *Mycobacterium avium* complex. *J. Immunol.* 140: 3006–3013.
- Appelberg, R., and I. M. Orme. 1993. Effector mechanisms involved in cytokine-mediated bacteriostasis of *Mycobacterium avium* infections in murine macrophages. *Immunology* 80: 352–359.
- Kindler, V., A.-P. Sappino, G. E. Grau, P.-F. Pigué, and P. Vassalli. 1989. The inducing role of tumor necrosis factor in the development of bactericidal granulomas during BCG infection. *Cell* 56: 731–740.
- Appelberg, R., A. G. Castro, J. Pedrosa, R. A. Silva, I. M. Orme, and P. Minópio. 1994. The role of γ interferon and tumor necrosis factor- α during the T cell independent and dependent phases of *Mycobacterium avium* infection. *Infect. Immun.* 62: 3962–3971.
- Appelberg, R., A. Sarmento, and A. G. Castro. 1995. Tumor necrosis factor α (TNF α) in the host resistance to mycobacteria of distinct virulence. *Clin. Exp. Immunol.* 101: 308–313.
- Ehlers, S. 2005. Tumor necrosis factor and its blockade in granulomatous infections: differential modes of action of infliximab and etanercept? *Clin. Infect. Dis.* 41: S199–S203.
- Locksley, R. M., N. Killeen, and M. J. Lenardo. 2001. The TNF and TNF receptor superfamilies: integrating mammalian biology. *Cell* 104: 487–5012.
- Smith, D., H. Hansch, G. Bancroft, and S. Ehlers. 1997. T-cell-independent granuloma formation in response to *Mycobacterium avium*: role of tumour necrosis factor- α and interferon- γ . *Immunology* 92: 413–421.
- Bean, A. G. D., D. R. Roach, H. Briscoe, M. P. France, H. Korner, J. D. Sedgwick, and W. J. Britton. 1999. Structural deficiencies in granuloma formation in TNF gene-targeted mice underlie the heightened susceptibility to aerosol *Mycobacterium tuberculosis* infection, which is not compensated for by lymphotoxin. *J. Immunol.* 162: 3504–3511.
- Ehlers, S., J. Benini, S. Kutsch, R. Endres, E. T. Rietschel, and K. Pfeffer. 1999. Fatal granuloma necrosis without exacerbated mycobacterial growth in tumor necrosis factor receptor p55 gene-deficient mice intravenously infected with *Mycobacterium avium*. *Infect. Immun.* 67: 3571–3579.
- Ehlers, S., S. Kutsch, E. Ehlers, J. Benini, and K. Pfeffer. 2000. Lethal granuloma disintegration in mycobacteria-infected TNFRp55^{-/-} mice is dependent on T cells and IL-12. *J. Immunol.* 165: 483–492.
- Flynn, J. L., M. Goldstein, J. Chan, K. J. Triebold, K. Pfeffer, C. J. Lowenstein, R. Schreiber, T. W. Mak, and B. R. Bloom. 1995. Tumor necrosis factor- α is required in the protective immune response against *Mycobacterium tuberculosis* in mice. *Immunity* 2: 561–572.
- Bekker, L.-G., A. L. Moreira, A. Bergtold, S. Freeman, B. Ryffel, and G. Kaplan. 2000. Immunopathologic effects of tumor necrosis factor α in murine mycobacterial infection are dose dependent. *Infect. Immun.* 68: 6954–6961.
- Bopst M., I. Garcia, R. Guler, M. L. Ollerros, T. Rulicke, M. Muller, S. Wyss, K. Frei, M. le Hir, and H.-P. Eugster. 2001. Differential effects of TNF and LT α in the host defense against *M. bovis* BCG. *Eur. J. Immunol.* 31: 1935–1943.
- Jacobs, M., N. Brown, N. Allie, and B. Ryffel. 2000. Fatal *Mycobacterium bovis* BCG infection in TNF-LT- α -deficient mice. *Clin. Immunol.* 94: 192–199.
- Zganiacz, A., M. Santossuoso, J. Wang, T. Yang, L. Chen, M. Anzulovic, S. Alexander, B. Gicquel, Y. Wan, J. Bramson, et al. 2004. TNF- α is a critical regulator of type I immune activation during intracellular bacterial infection. *J. Clin. Invest.* 113: 401–413.
- Garcia, I., Y. Miyazaki, G. Marchal, W. Lesslauer, and P. Vassalli. 1997. High sensitivity of transgenic mice expressing soluble TNFR1 fusion protein to mycobacterial infections: synergistic action of TNF and IFN- γ in the differentiation of protective granulomas. *Eur. J. Immunol.* 27: 3182–3190.
- Flórido, M., and R. Appelberg. 2004. Granuloma necrosis during *Mycobacterium avium* infection does not require tumor necrosis factor. *Infect. Immun.* 72: 6139–6141.
- Aggarwal, B. B. 2003. Signalling pathways of the TNF superfamily: a double-edged sword. *Nat. Rev. Immunol.* 3: 745–756.
- Zakharova, M., and H. K. Ziegler. 2005. Paradoxical anti-inflammatory actions of TNF- α : inhibition of IL-12 and IL-23 via TNF receptor I in macrophages and dendritic cells. *J. Immunol.* 175: 5024–5033.
- Flórido, M., J. E. Pearl, A. Solache, M. Borges, L. Haynes, A. M. Cooper, and R. Appelberg. 2005. γ Interferon-induced T-cell loss in virulent *Mycobacterium avium* infection. *Infect. Immun.* 73: 3577–3586.
- Flórido, M., A. M. Cooper, and R. Appelberg. 2002. Immunological basis of the development of necrotic lesions following *Mycobacterium avium* infection. *Immunology* 106: 590–601.
- Ehlers, S., J. Benini, H. D. Held, C. Roeck, G. Alber, and S. Uhlig. 2001. $\alpha\beta$ T cell receptor-positive cells and interferon- γ , but not inducible nitric oxide synthase, are critical for granuloma necrosis in a mouse model of mycobacteria-induced pulmonary immunopathology. *J. Exp. Med.* 194: 1847–1859.
- Pais, T. F., J. F. Cunha, and R. Appelberg. 2000. Antigen specificity of T-cell response to *Mycobacterium avium* infection in mice. *Infect. Immun.* 68: 4805–4810.
- Atochina, O., T. Daly-Engel, D. Piskorska, E. McGuire, and D. A. Harn. 2001. A schistosome-expressed immunomodulatory glycoconjugate expands peritoneal Gr1⁺ macrophages that suppress naive CD4⁺ T cell proliferation via an IFN- γ and nitric oxide-dependent mechanism. *J. Immunol.* 167: 4293–4302.
- Mordue, D. G., and L. D. Sibley. 2003. A novel population of Gr1⁺-activated macrophages induced during acute toxoplasmosis. *J. Leukocyte Biol.* 74: 1015–1025.
- Ehrlich, S., C. Infante-Duarte, B. Seeger, and F. Zipp. 2003. Regulation of soluble and surface-bound TRAIL in human T cells, B cells, and monocytes. *Cytokine* 24: 244–253.